

Studying the Impact of Transportation During Lockdown on the Spread of COVID-19 Using Agent-Based Modeling

Shikha Bhat^{*a}, Ruturaj Godse^{*b}, Shruti Mestry^{id}^c and Vinayak Naik^{id}^d

BITS Pilani, Goa, India

Keywords: Agent-Based Simulation, COVID-19, Artificial Intelligence.

Abstract: The COVID-19 pandemic has posed challenges for governments concerning lockdown policies and transportation plans. The exponential rise in infections has highlighted the importance of managing restrictions on travel. Previous research around this topic has not been able to scale and address this issue for India, given its diversity in transportation networks and population across different states. In this study, we analyze the patterns of the spread of infection, recovery, and death specifically for the state of Goa, India, for twenty-eight days. Using agent-based simulations, we explore how individuals interact and spread the disease when traveling by trains, flights, and buses in two significant settings - unrestricted and restricted local movements. Our findings indicate that trains cause the highest spread of infection within the state, followed by flights and then buses. Contrary to what may be assumed, we find that the effect of combinations of all modes of transport is not additive. With multiple modes of transport activities, the cases rise exponentially faster. We present equivalence points for the number of vehicles running per day in unrestricted and restricted movement settings, e.g., one train a day in unrestricted movement spreads the disease as eight trains a day in restricted movement.

1 INTRODUCTION

In recent years, the world has faced innumerable challenges posed by the Severe Acute Respiratory Syndrome CoronaVirus 2 (SARS-CoV-2), also known as COVID-19. The disease spreads from one infected individual to another through respiratory droplets and physical contact. Due to a lack of awareness, research, and interventions during the initial outbreak, the virus rapidly spread to over a hundred countries within three months, compelling the WHO to declare a global pandemic on March 11, 2020.

To prevent a similar disease from spreading in this fashion, we urgently need to study the disease spread using epidemiological modeling techniques. Mathematical models involve constant values that determine only one outcome. In contrast, computer simulations that consist of agent-based models are stochastic and have a better chance of mimicking reality. An agent-based model involves agents as autonomous entities

and an environment in which the agents interact with each other to portray any real-life system.

India was one of the most affected countries in the world. Goa, a state in India, had a test positivity rate of five times the national average. This paper presents an agent-based simulation created in NetLogo software (net, 1999) that helps us design an epidemiological model incorporating spatial data of population and transportation. Using the model, we estimate the spread of COVID-19 in Goa through railway, road, and airway transportation networks. The agents are simulated as individuals interacting with each other as they travel via the transportation networks and unfold the spread of the infection with time. We simulate the transportation networks with varying frequency, introduce restrictions on local movements, and measure the rise in the population's number of infections and recoveries. Using the simulation, we get an insight into specific details, such as an upper bound on vehicles required to minimize the disease spread, the rate of change of infections, and the impact of the restriction on movement, i.e., lockdown. The model will help the general public perceive the best-case to worst-case scenarios under different degrees of movement. Our study will help policymakers to propose effective strategies to minimize the disease's spread.

^a  <https://orcid.org/0000-0002-3989-2005>

^b  <https://orcid.org/0000-0002-1091-4311>

^c  <https://orcid.org/0000-0001-9672-1635>

^d  <https://orcid.org/0000-0003-3637-2167>

* These authors contributed equally to this work.

We validate the model by comparing it with real-world data.

In the following sections, we describe past research efforts to create pandemic models, clearly lay out the problem statements we address, and the methodology we use to approach the problem. Later sections discuss the details of our implementation of the methods, and we then present the results obtained from the simulation model. The conclusion summarizes the paper and discusses ways the presented work can be extended further.

2 RELATED WORK

The COVID-19 global pandemic has urged researchers to study the infection spread to implement appropriate lockdown policies and other non-pharmaceutical interventions. Modeling the pandemic in a simulation, analyzing how the infection spreads among people, and watching the patterns emerge are effective ways to study the pandemic. Previous works can broadly be classified into deterministic and stochastic modeling. Our study uses agent-based modeling, which is a sub-category of stochastic modeling. These methods are detailed as follows.

2.1 Deterministic Modeling

Deterministic modeling attempts to study some part (or form) of a real-life problem in mathematical terms. Previously, there have been many studies that mathematically model the COVID-19 outbreak. These models are deterministic, ranging from simple math (Tang and Wang, 2020) to nonlinear differential equations (Iboi et al., 2020) to fractional order mathematical modeling (Ahmad et al., 2020). Deterministic epidemic models, such as the Susceptible, Exposed, Infected, and Recovered (SEIR) model (Carcione et al., 2020)(Reiner et al., 2021), are useful tools in epidemiology. However, despite the many advantages of deterministic models, it can be difficult to include realistic population networks in such models. Thus, we usually use the SEIR techniques in combination with some stochastic parameters to create a better model of the real situation (Omar et al., 2021).

2.2 Stochastic Modeling

Purely mathematical modeling of a complex situation, such as a pandemic, often cannot accurately represent a real-world scenario. In the past, there have been efforts to produce stochastic processes to quantitatively

reproduce the spread of a pandemic and the number of infections.

Mainly three types of stochastic epidemic simulations have been explored. The first builds on mathematical ODE deterministic models by using stochastic differential equations (Zhang et al., 2020). The second method is the Markov Chain Monte Carlo method, where the probability of each possible event is assessed at each time step, and one of the events is chosen randomly (weighted by its probability of occurrence) (Chatterjee et al., 2020). Using a Monte Carlo simulation model, Bartsch et al. (Bartsch et al., 2022) compared what would happen if face masks were used versus not used until the population gets their final vaccination. The third and final approach is agent-based models with stochastic parameters, in which each agent behaves in certain ways to understand the underlying movements and interactions between individuals. Wilder et al. (Wilder et al., 2020) developed a stochastic SEIR agent-based model for the spread of SARS-CoV2 and discusses the role of age distribution and family structure in the model. Our study uses agent-based modeling to understand the spread of the disease among locals and passengers traveling via different transportation methods.

Other aspects of our paper include the geospatial representation of a state, restrictions on local movement, and the effect of transportation networks on the disease spread. Previously, Koo et al. (Koo et al., 2022) created an agent-based model, GeoDEMOS-R, incorporating a geographical, demographic, and epidemiological model of Singapore for respiratory diseases. We simulate time-specific restrictions on the movement in the lockdown scenario. We use QGIS and NetLogo to simulate a geospatial environment of Goa.

The research on the spread of COVID-19 through transportation networks in India, while comparing the restrictions on local movement, is limited. Talekar et al. (Talekar et al., 2020) implemented cohort strategies on top of a city-scale agent-based epidemic simulator. They mapped the agents on a geospatial network and studied the effect of grouping agents together in travel in Mumbai railways. Our simulation-based model treats each agent as an autonomous individual living in restricted and unrestricted lockdown scenarios. In our study, we model trains, flights, and buses separately and find that they differ greatly in terms of infection spread. Compared to their study of the effect of creating cohorts on the spread via only train, our study is broader. We focus on how we can better the transportation and lockdown policies in a state, using the information collected via the agent-based simulation.

3 PROBLEM STATEMENTS

In favor of allowing socio-economic activities, it is essential to understand how the infection spreads via the transport networks in the state. This will help in planning efficient rules and regulations in lockdown and provide insight into predicting the future of the outbreaks. To that end, the aims of the simulation study are as follows.

1. Measure the cumulative number of infections while varying the frequency of each mode of transport
2. Measure the total number of recoveries while varying the frequency of each mode of transport
3. Find an upper bound on the number of transport vehicles allowed to run while keeping the maximum number of infections less than 20%
4. Measure the rate of change, as calculated in the following equation, in the number of infections for the initial days of the disease spread vis-à-vis the final days

$$\frac{(b-a)}{a} * 100 \quad (1)$$

where a is the number of infected or recovered or deceased people for a day, and b is the number of infected or recovered or deceased people for the following day

5. Compare different frequencies of transportation during two scenarios of movements, which produce an equivalent number of infections within twenty-eight days
6. Validate the model by comparing and correlating it with real-world data

4 METHODOLOGY AND IMPLEMENTATION

We describe our methodology and give details of implementing our agent-based model using the data in this section.

4.1 GIS Data Collection

Goa is connected to the other states of India by railways, airways, and roadways. We collect datasets for these transportation networks in Goa from OpenStreetMap using QGIS software (QGIS Development Team, 2021) and generate desired shapefiles for the model. These files contain vector point data for nine railway stations along the Konkan railway route, one

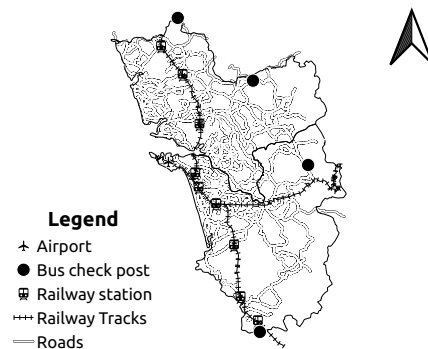


Figure 1: A map showing the railway stations, bus check-posts, airport and transportation networks inside Goa.

airport at Dabolim, and four border-crossing points on the national highways. We show the locations of stops for all three modes in Figure 1.

We gather the rail, road, and air-related data (tra, 2022) to set up variable values such as the maximum number of trains or the number of passengers onboard. The rail-related data includes trains' numbers, routes, timings, and frequency. The airway-related data consists of all the airlines operating in Goa, with the timings and frequency of flights. The road-related data comprises the number of buses running from Goa to Maharashtra and Goa to Karnataka via different entry points. We use the vector polygon datasets for administrative boundaries to ensure the agents move within the representative GIS space. The data for COVID-19 statistics and the nationwide lockdown policy timeline help us calibrate and validate our model at the end.

4.2 Agent-Based Model

We elaborate on the three main simulation model components - the agents, the environment in which the agents live and travel, and the interaction between the agents that result in disease transmission.

4.2.1 Agents

To simulate the COVID-19 disease's spread among humans, we create agents representing the human population of Goa in the GIS space. We use a scaled-down population of Goa to create the total number of agents in each district of Goa. The people in the districts can move around, get in and out of the trains, flights, or buses, get exposed to the disease, and infect other people. We define the people currently in the state as a class of *persons* and those traveling via train, flight, or bus as a class of *passengers*. The 'per-

sons' own a district variable that allows us to track the district they belong to, and the 'passengers' own a vehicle variable, such as flight or train number. The passenger's location changes with the vehicle's location.

4.2.2 Environment

This study focuses on creating an environment mimicking Goa's transportation network via rail, road, and air. We insert the vector datasets for administrative boundaries, railway stations, airports, and highway checkpoints to achieve that. The state boundaries are loaded to ensure the confinement of agents within the GIS space. We define trains that use the Konkan Railway route running through Goa from Pernem station in the North Goa district to Loliem station in the South Goa district. Dabolim airport denotes the location for flights to arrive and depart. Highway check posts are the entry points at the Goa border to facilitate bus travel. We use the projected coordinate system EPSG:779 for the state of Goa.

4.2.3 Interaction

Our model employs the "SEIRD" framework model, distinguished as Susceptible - Exposed - Infected - Recovered - Deceased, demonstrating the disease progression in individual agents. Among all the different types of epidemic modeling, the SEIRD framework is the most extensive, keeping track of every stage. We allow individuals to travel, and while they move, they come in contact with each. Their interaction unfolds the disease transmission. Each individual is assigned a variable that tracks her state of disease progression in terms of S-E-I-R-D. At the start of the simulation, some individuals are infected, and others are all susceptible to the disease. As the individuals move around and come in contact with others, they are exposed to the disease, and after some time, given some infection chances, they are infected with the disease. After a recovery period, the infected individuals either recover or continue to remain infected, depending on the recovery chances. At this point, the chances of death are also checked. If the infected individuals die, they are removed from the simulation.

4.3 Implementation

We simulate all three modes of transport – trains, flights, and buses, individually and in combination. For each mode, we initialize the vehicles to their starting locations and let people in the district become passengers that board these vehicles. We update the vehicle's and passenger's positions every hour and

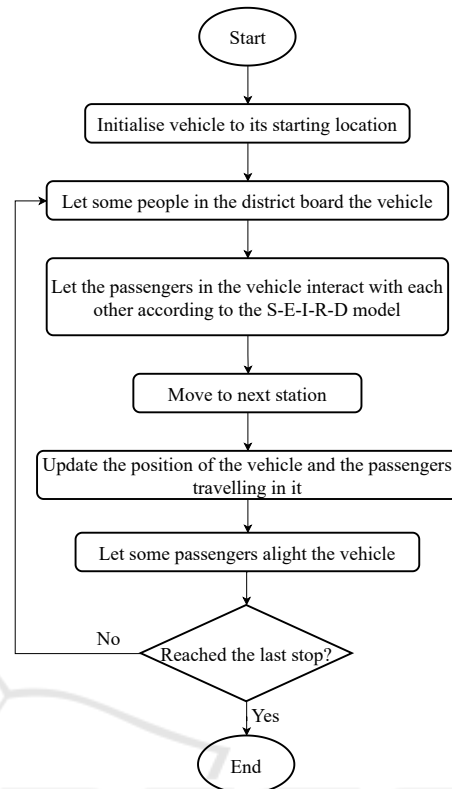


Figure 2: Flowchart for the simulation of one vehicle. Multiple such vehicles run in parallel, with different stations and start times.

let the passengers interact with each other using the SEIRD model. New passengers board the vehicle, and the old passengers alight the vehicle at different stations/ports. Then, the people who alight at these stations travel home. The flowchart explaining the simulation course for a vehicle is shown in Figure 2. We run multiple such vehicles simultaneously from different stations and at different times, following the transportation data obtained.

People outside the vehicles randomly mingle in their districts and interact, spreading infection within a specified radius. We build the simulations representing the movement of people in two ways. In the first scenario with *unrestricted movement*, we allow the individuals to move within the state and utilize the transportation networks for inter-state travel. The second scenario with *restricted movement* allows inter-state travel but restricts local movement. These are the two movements allowed in India during the COVID-19 period. We only monitor people in the state and remove those traveling out of the state, via flights and buses, from our simulation.

Platform. We select the NetLogo software as our modeling platform for its diverse characteristics and

tools. The GIS extension provided by NetLogo enables the model to accommodate vector as well as raster GIS data. It is an object-oriented agent-based model, where each agent is an object. The monitors, GIS space, and plots update at every tick, and the results are tracked. A tick corresponds to an hour in our simulation. We execute the model without using GUI on a Red Hat Linux server. BehaviorSpace, an inbuilt tool in NetLogo, allows us to execute multiple simulations in parallel by use of threading. The BehaviorSpace-based simulation of our model is called through the command line using a NetLogo-headless batch file which executes each simulation for a different set of parameters, and the output is exported as CSV files. We average the results over three runs of the experiments and then plot graphs using MATLAB.

Input Parameters. To study each transport network's effect on the spread of the disease, we simulate the model separately for railways, airways, and roadways, and then for all of the transport networks combined. The numbers of vehicles and passengers are extracted from real-world data. We downscale the population of Goa to 1%, which results in 15,000 individuals in the model. The number of people in each vehicle is scaled down by a factor of 10. We simulate for twenty-eight days to capture the consequent recoveries and fatalities. The parameters for the simulation, vehicles, and their respective values are given in Table 1 and 2.

Table 1: Parameters for the agent-based simulation.

Parameter	Value
Time period	28 days
Population	15,000
Chances of exposure	70%
Exposure radius	0.001 units (~33.85 metres)
Incubation period	4 days
Illness period	10 days
Chances of infection	70%
Chances of recovery	80%
Chances of death	5%

5 RESULTS

We simulate agent-based models for trains, flights, buses, and a combination of these modes. We conduct each simulation with different seed values three times and average the results.

5.1 Cumulative Number of Infections with Varying Frequency for Transportation

5.1.1 Trains

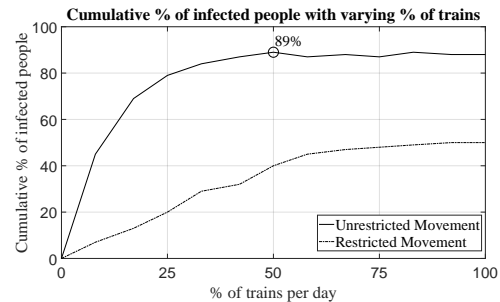


Figure 3: The cumulative percentage of infected people with an increasing number of trains running per day for unrestricted and restricted movements. The cumulative number increases until we reach a saturation point of 89% with more than 50% trains per day in the case of unrestricted movement.

Figure 3 shows that unrestricted movement results in 45% to 89% of the population contracting the disease, with 8% to 50% of trains running daily, respectively. On average, the cumulative number increases at 17% with an increase in the percentage of trains until 25% of the trains. This rate decreases to 3.3% from 25% to 50% of trains. With more than 50% of trains per day, it produces nearly the same cumulative percentage of infections in the range of 87% to 89%.

When the local movement is restricted, we observe that the cumulative number of infections is 7% with 8% of trains and 50% with 100% of trains running daily. Until 50% of trains per day, there is an average increase of 6.6%. The increase is 1.8% with a further rise in the number of trains. The restrictions with more than 50% of trains result in nearly half of the population getting the disease. However, we observe that the restriction on the local movement with 100% of trains lowers the cumulative number to 38% as compared to the unrestricted movement. To reduce the cumulative number, the trains need to be operated with restricted local movement.

5.1.2 Flights

Figure 4 shows that an increase in the percentage of flights with unrestricted movement results in up to 63% of the population getting infected in twenty-eight days. In contrast to the trains, the cumulative number of infections increases at 1% from 10% to 30% of trains. The rate further increases to 8.2% for more than 30% of flights.

Table 2: Parameters for each mode of transport in the simulation.

Mode of Transport	Number of Vehicles	Number of Passengers
Trains	[1, 2, 3, 4, 5, 6, 7, 8, 9, 10, 11, 12]	50
Flights	[10, 20, 30, 40, 50, 60, 70, 80, 90, 100]	9
Buses	[30, 60, 90, 120, 150, 180, 210, 240, 270, 300]	5

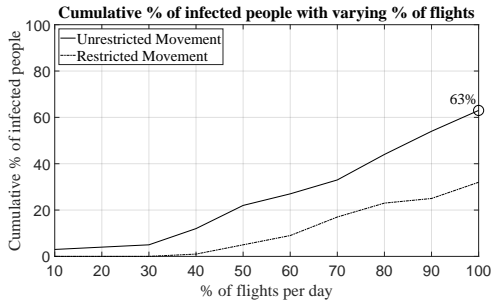


Figure 4: The cumulative percentage of infected people with an increasing number of flights flying per day for unrestricted and restricted movements. In the case of unrestricted movement, the number of infections keeps rising up to 63%.

In the case of restricted local movement with 10% to 30% of flights, the cumulative percentage of infected people remains less than 1%. We see that 1% of the population gets the infection with 40% of flights. With a further increase in flights to 100%, we observe that 32% of the population contracts the infection. On average, with more than 40% of flights per day, the cumulative number increases at 5.1%. The difference in cumulative numbers between the unrestricted and restricted movements rises with an increase in the percentage of flights suggesting that, unlike trains, restrictions on local movement are benefiting even if the percentage of flights is more than 50%.

5.1.3 Buses

In Figure 5, we observe that buses, among other transport modes, result in the least number of cumulative infections even. The unrestricted movement shows 3% to 27% of the population getting infected with 10% to 100% of buses, respectively. We see an increase of 1% from 10% to 50% of buses. It increases at 4% from 60% to 100% of buses.

Similar to the case of flights, the restricted local movement with 10% to 30% of buses shows less than 1% of the infected population. The cumulative number for 40% to 90% of buses increases at 2.6%. After 90%, the rate is 9%. As the cumulative % with unrestricted movement is 27%, it is unsafe to operate buses with full frequency without local restrictions.

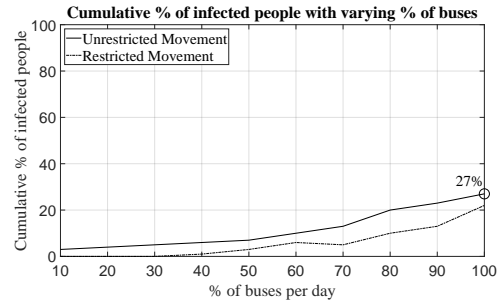


Figure 5: The cumulative percentage of infected people with an increasing number of buses running per day for unrestricted and restricted movements. The number of infections keeps rising to 27% for the case of unrestricted movement.

5.1.4 Combination

The combination of all transport modes shows the worst scenario regarding the infected population. In Figure 6, we observe that the unrestricted movement results in 90% of the population getting infected with 10% of vehicles and the whole population with 40% of vehicles.

With restrictions on local movement, we see that 68% of the population gets infected with 10% of vehicles. The restriction in local movement lowers the cumulative percentage but is not significant enough to contain the infection. The whole population contracts the disease when more than 50% of vehicles operate. This suggests that operating the transport network simultaneously transmits the infection the most.

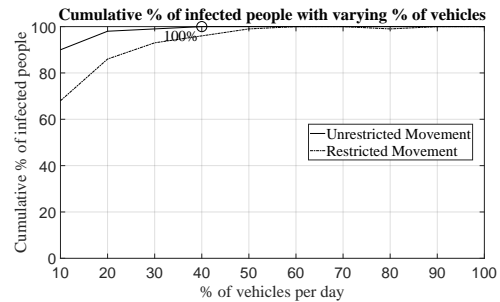


Figure 6: The cumulative percentage of infected people with an increasing number of vehicles running per day for unrestricted and restricted movements. In the case of unrestricted movement, The number of infections reaches 100% with more than 40% of vehicles.

5.2 Number of Recoveries with Varying Frequency of Transportation

5.2.1 Trains

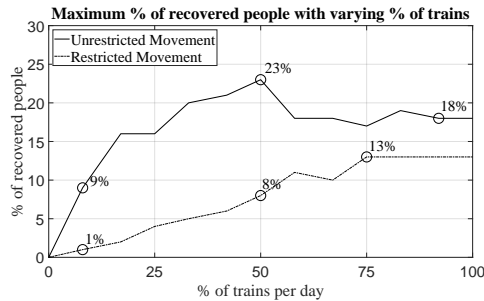


Figure 7: The maximum number of recoveries with increasing trains running per day for unrestricted and restricted movements scenarios. The percentage of the population recovering each day increases until 50% trains per day, after which it remains nearly constant.

The maximum number of recovered people observed within twenty-eight days is 23% of the total population, with 50% trains, i.e., six trains running per day in case of unrestricted movement as shown in Figure 7. The percentage of the population recovering each day increases from 9% to 23% for unrestricted movement and from 1% to 8% for restricted movement as the number of trains increases up to 50% trains, which is six trains per day. After that, it remains almost constant at 13% and at 18% for further increase in the number of trains for restricted and unrestricted movements, respectively. The number of recoveries increases faster initially with an increase in trains and later flattens. As the number of infected people increases from 36% with one train to 71% with twelve trains, as shown in Figure 11, we see an increase in the number of recovered people from 9% to 18%, respectively. It implies that the higher the frequency of trains, the higher the number of infections in a short period which, if people recover, leads to an increase in the number of recoveries.

5.2.2 Flights

In Figure 8, we observe that the maximum number of recovered people within twenty-eight days is 18% of the total population, with 100% flights, i.e., a hundred flights running per day, for unrestricted movement. The number of recoveries increases steadily with flights for unrestricted and restricted movements. In the case of unrestricted movement, from 10% to 30% of flights, we see 1% of the population recover. With 40% to 70% of flights, the rate rises from 2% to 6% of the population to recover. With more than 70%

of flights, the rate further rises from 11% to 18%. For restricted movement, the number of recoveries ranges from 1% to 12% for 10% to 100% of flights. From the number of infections, we know that restricted movement minimizes the infection from spreading, allowing people to recover. This, in turn, buys time for healthcare facilities to be ready.

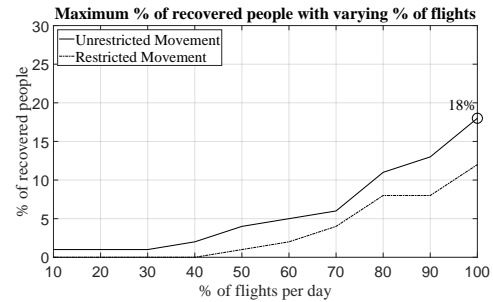


Figure 8: The maximum number of recoveries with an increasing number of flights running per day for unrestricted and restricted movements scenarios. The number of recoveries increases steadily with the number of flights.

5.2.3 Buses

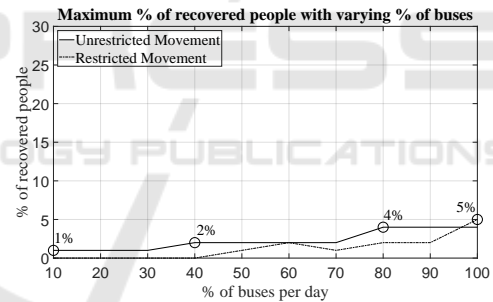


Figure 9: The maximum number of recoveries with an increasing number of buses running per day for unrestricted and restricted movements. The number of recoveries remains constant up to two hundred and ten buses per day, after which it increases in the case of unrestricted movement. The case of restricted movement produces almost the same number of recoveries as that of unrestricted.

We observe the maximum number of recovered people within twenty-eight days, as shown in Figure 9, to be 5% of the total population, with 100% buses, i.e., three hundred buses per day in case of unrestricted movement. The number of recoveries remains constant at 1-2% for up to two hundred and ten buses per day, after which it increases to 4% for the case of unrestricted movement. With an increase in the frequency of buses, the restricted movement produces a similar number of recovered people as the unrestricted movement. Thus, buses are the most favorable transport mode in minimizing infec-

tions even with 100% of frequency without restricting local movement.

5.2.4 Combination

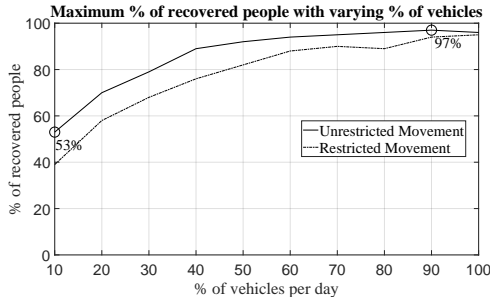


Figure 10: The maximum number of recoveries is 97% of the total population. It is observed with eleven trains, ninety flights, and two hundred and ten buses running per day for unrestricted movement at 97% of the total population.

With 90% of total vehicles, i.e., eleven trains, ninety flights, and two hundred and ten buses running per day, for unrestricted movement, the maximum number of recovered people observed within twenty-eight days is 97% of the total population as shown in Figure 10. The number of recoveries keeps increasing from 53% to 97% as the frequency of each transport mode increases and reaches the maximum. We observe that with an increase in the frequency of vehicles, the numbers of recovered people for restricted and unrestricted are nearly equal. Allowing all transport modes to operate together leads to a rapid increase in the spread of infection. Thus, a combination of transport networks must be avoided regardless of restrictions on the local movement.

5.3 An Upper Bound On the Number of Vehicles To Keep the Maximum Number of Infections Less Than 20%

5.3.1 Trains

With 8% of trains, as shown in Figure 11, the maximum number of infections goes up to 36% in case of unrestricted movement. Thus, we cannot allow trains to run with unrestricted movement if we want to keep the maximum number of cases less than 20%. In the case of restricted movement, we can allow up to 25% trains per day.

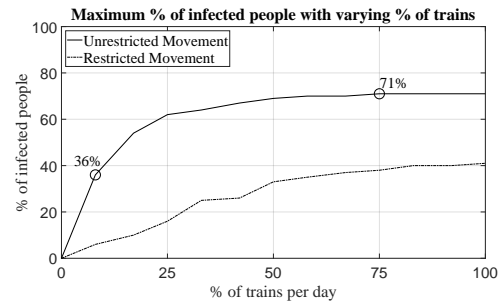


Figure 11: We show the maximum number of infected people with an increasing number of trains running per day for unrestricted and restricted movements. The number of infections keeps rising until we reach a saturation point of 71% once we allow more than 75% trains per day.

5.3.2 Flights

In Figure 12, we see that the maximum number of infections stays below 20% for up to 50% of flights per day in case of unrestricted movement. In restricted movement, the maximum number of infections remains below 20% even for the maximum frequency of flights.

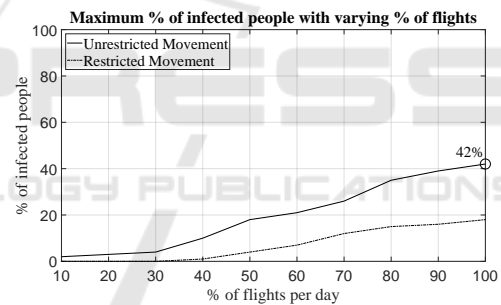


Figure 12: We show the maximum number of infected people with an increasing number of flights running per day for the scenarios of unrestricted and restricted movements. The number of infections keeps rising for twenty-eight days, and we see a considerable increase of ~ 5% for cases each time as we increase the number of flights per day by ten.

5.3.3 Buses

In the case of unrestricted movement, the number of infections in Figure 13, stays below 20% till 90% of buses per day. With the maximum frequency of buses, the number of infections rises to 23%. In case of restricted movement, the maximum number of infections stays below 20% even for the maximum frequency of buses.

5.3.4 Combination

With the combination of the least frequency for each transportation mode, i.e., three trains, ten flights, and

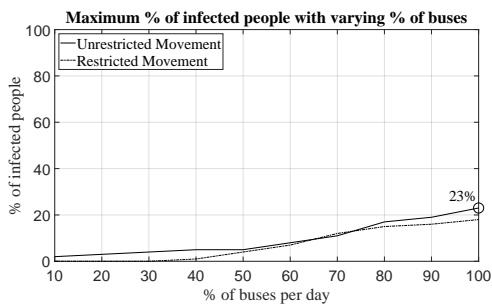


Figure 13: We show the maximum number of infected people with an increasing number of buses per day for both unrestricted and restricted movement scenarios. The number of infections keeps rising for twenty-eight days. With fewer buses, the number of infections increases steadily (~1%) each time we increase the frequency by ~10%, but as the number of buses crosses ~50% (150), we see a sharp increase.

thirty buses, the minimum number of infections, as shown in Figure 14, is 57% in case of unrestricted movement and 40% in case of restricted movement. Thus, we cannot allow a combination of transports if we do not want the maximum number of cases to go above 20%.

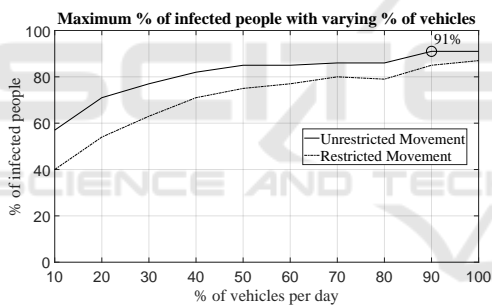


Figure 14: We show the maximum number of infected people with an increasing number of buses per day for both unrestricted and restricted movement scenarios. We see the maximum number of infections for twelve trains, hundred flights, and three hundred buses running per day in unrestricted movement. It is 91% of the total population.

5.4 Rate of Change in Number of Infection for the Initial Days vis-à-vis Final Days

5.4.1 Trains

In Figure 15, we observe that the number of infections rose by 235% and 192% on the fifth day with twelve trains per day for unrestricted and restricted movement, respectively. Since the incubation period is the first four days, we see a sharp increase in the number

of infections during that period. The growth decreases rapidly the next day and eventually goes to zero, suggesting that the number of infections decreases and starts falling as more people recover.

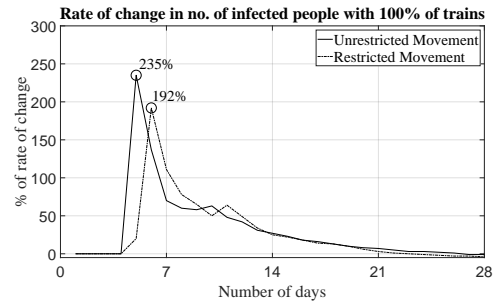


Figure 15: We show the rate of change in the number of infections over a period of twenty-eight days when twelve trains operate per day.

5.4.2 Flights

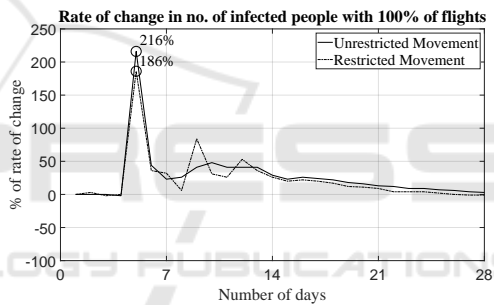


Figure 16: We show the rate of change in the number of infections over twenty-eight days when a hundred flights are operated per day.

In Figure 16, we see that the number of infections rose by 216% and 186% on the fifth day with hundred flights per day for unrestricted and restricted movement, respectively. Similar to the case of trains, this growth falls rapidly after the incubation period. Eventually, it goes to zero, suggesting that the number of cases eventually saturates and starts falling as more people recover.

5.4.3 Buses

In Figure 17, we do not see a sudden increase in the rate of change for the number of infections even with the maximum frequency of the buses. The rate of change for the number of infections remains between 25-50% for most days. This suggests that the spread of infection, in the case of buses, is much more controlled than on trains and flights.

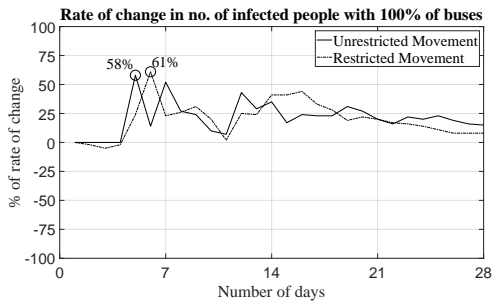


Figure 17: We show the rate of change in the number of infections over twenty-eight days when three hundred buses operate per day.

5.4.4 Combination

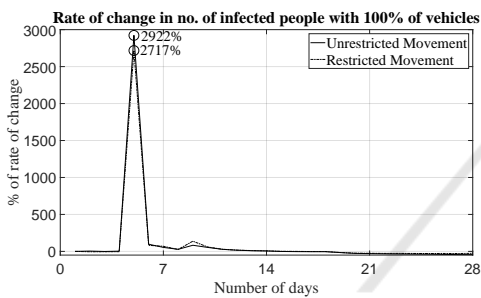


Figure 18: We show the rate of change in the number of infections over twenty-eight days when twelve trains, hundred flights, and three hundred buses operate per day.

In Figure 18, we see that the number of infections rose by 2922% and 2717% on the fifth day with twelve trains, hundred flights, and three hundred buses per day for unrestricted and restricted movement, respectively. This is more than twelve times the rise in infections for any individual mode of transport with unrestricted movement and more than fourteen times in case of restricted movement. Thus, we see that a combination of the three modes of transport grows faster than linear.

5.5 Equivalence Point between Unrestricted and Restricted Movements

5.5.1 Trains

Figure 19 (a) and Figure 19 (b) show that the scenario of unrestricted movement of people with one operational train per day produces an equivalent number of infections as the scenario of eight operational trains per day but with restricted movement.

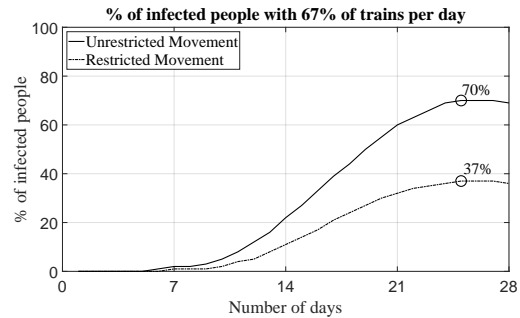
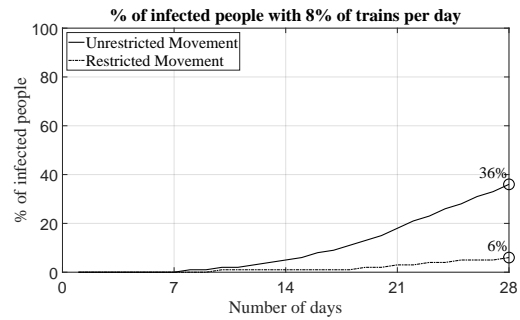


Figure 19: We show an equivalence point between unrestricted movement and restricted movement for trains. (a) The scenario of 8% of trains with unrestricted movement shows a peak of 36% of the population to be infected. (b) The scenario of 67% of trains with restricted movement shows a peak of 37% of the population to be infected.

5.5.2 Flights

Figure 20 (a) and Figure 20 (b) show the unrestricted movement of people with fifty operational flights per day produces an equivalent number of infections as the scenario of hundred operational flights per day but with restricted movement.

5.5.3 Buses

The scenario of unrestricted movement of people with two hundred and forty operational buses per day, as shown in Figure 21 (a), produces an equivalent number of infections as the scenario of three hundred operational buses per day but with restricted movement a shown in Figure 21 (b).

5.5.4 Combination

The scenario of unrestricted movement of people with 30% of vehicles, as shown in Figure 22 (a), produces an equivalent number of infections as the scenario of 60% of vehicles per day but with restricted movement, as shown in Figure 22 (b).

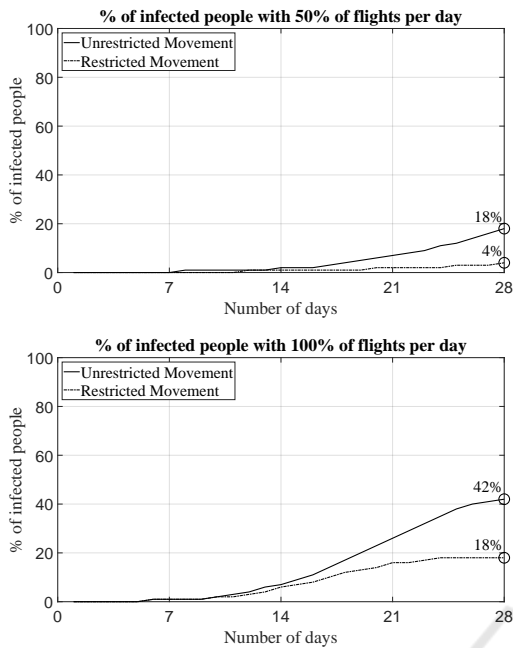


Figure 20: We show an equivalence point between unrestricted movement and restricted movement for flights. (a) The scenario of 50% of flights with unrestricted movement show shows a peak of 18% of the population to be infected. (b) The scenario of 100% of flights show shows a peak of 18% of the population to be infected.

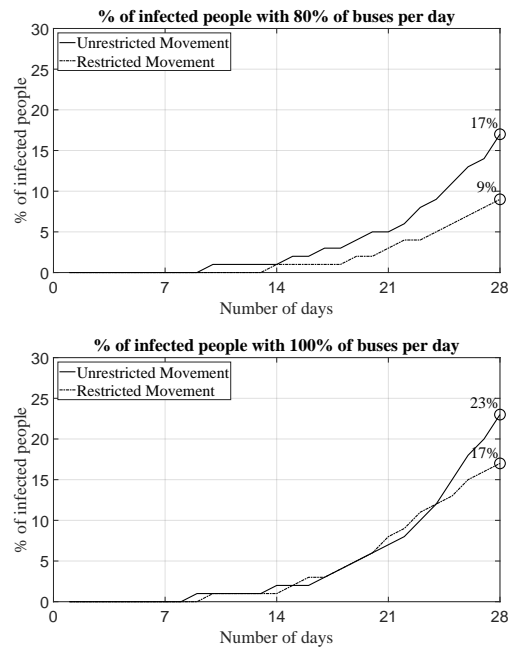


Figure 21: We show an equivalence point between unrestricted movement and restricted movement for buses. (a) The scenario of 80% of buses with unrestricted movement show shows a peak of 17% of the infected population. (b) The scenario of 100% of buses with restricted movement show shows a peak of 17% of the infected population.

5.6 A Comparison of Simulation Data with the Real-world Data

By plotting the results of the combined transportation, we find that it produces a bell-shaped curve. In Figure 23, we compare our simulation observations for the combined transportation with the real-world COVID-19 data for all three pandemic waves in Goa for twenty-eight days. The first wave begins in early November 2020, the second wave begins in early May 2021, and the third wave begins in the second week of January 2022. We plot the number of infections normalized individually per the maximum number of infections. The cases spread less rapidly as we go from the first wave to the third wave. We see that the curve for the unrestricted scenario reaches a maximum on the same timeline as the second wave. The curve for the restricted scenario reaches a maximum on the same timeline as the first wave and the third wave. While there were strict restrictions at the time of the first and third waves, the restrictions were lesser at the time of the second wave.

6 CONCLUSION AND FUTURE WORK

The spread of COVID-19 infections depends on several factors. This study presented how the infections spread via transportation networks in two different scenarios of movements allowed. This was done using the agent-based simulation modeling technique in NetLogo, combined with the geospatial representation of Goa and its railway stations, airports, and bus stop. Our source code and data files are publicly available at a GitHub ¹ repository.

Previous closely related work looking at the impact of transportation on the spread of the disease by Talekar et al. (Talekar et al., 2020) focused on how impactful the policy of creating cohorts of people is. We, however, look at every person as an individual and then measure how their movement via different transportation modes will impact the spread.

In the future, this simulation can be extended to multiple states and include international travel. More precise road movements of people can be tracked and

¹<https://github.com/Networked-Systems-Lab/Simulating-COVID-19-Using-ABM>

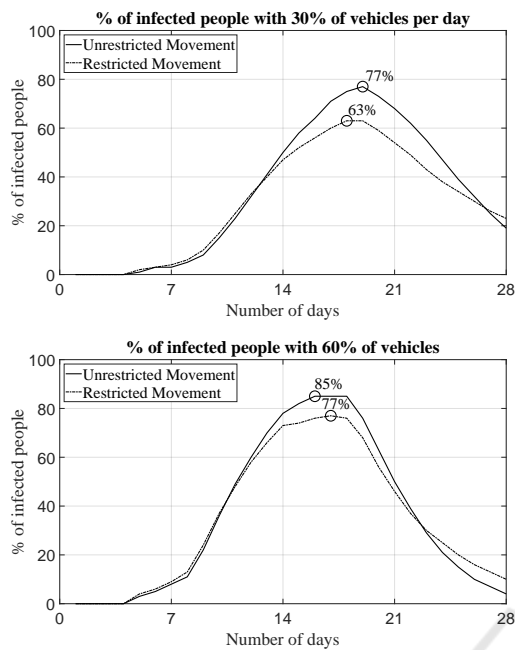


Figure 22: We show an equivalence point between unrestricted movement and restricted movement for the combination of transport modes. (a) The scenario of 30% of vehicles with unrestricted movement shows a peak of 77% in the number of infections. (b) The scenario of 60% of vehicles with restricted movement shows a peak of 77% in the number of infections.

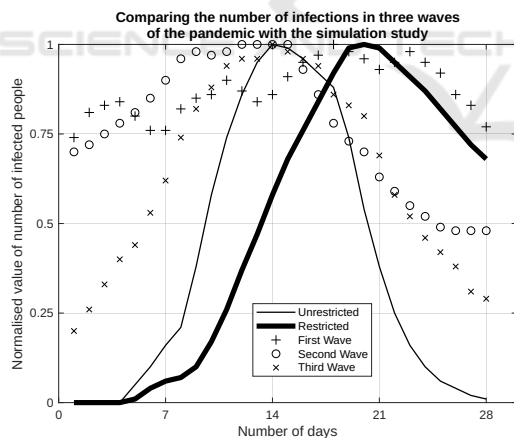


Figure 23: A comparison of our combined transportation simulation results to the three waves of COVID-19 in Goa. The peak of the second wave resembles the case of unrestricted and the peak of the third wave resembles that of restricted movement. This is a positive indicator for the accuracy of the simulation as cases rose less rapidly for the third wave, similar to the case of restricted movement.

used to identify exposure to the virus. This will require much more computation power as we need to track each person's and vehicle's movement. We may add vaccinated people to the simulation, who will

have immunity or fewer chances of getting the disease.

REFERENCES

(1999). Netlogo. <http://ccl.northwestern.edu/netlogo/>.

(2022). Transportation - department of tourism, government of goa. <https://goatourism.gov.in/transportation/>.

Ahmad, S., Ullah, A., Al-Mdallal, Q. M., Khan, H., Shah, K., and Khan, A. (2020). Fractional order mathematical modeling of covid-19 transmission. *Chaos, Solitons & Fractals*, 139:110256.

Bartsch, S., O'Shea, K., Chin, K., Strych, U., Ferguson, M., Bottazzi, M., Wedlock, P., Cox, S., Siegmund, S., Hotez, P., and Lee, B. (2022). Maintaining face mask use before and after achieving different covid-19 vaccination coverage levels: a modelling study. *The Lancet Public Health*, 7.

Carcione, J. M., Santos, J. E., Bagaini, C., and Ba, J. (2020). A simulation of a covid-19 epidemic based on a deterministic seir model. *Frontiers in Public Health*, 8.

Chatterjee, K., Chatterjee, K., Kumar, A., and Shankar, S. (2020). Healthcare impact of covid-19 epidemic in india: A stochastic mathematical model. *Medical Journal Armed Forces India*, 76(2):147-155.

Iboi, E., Sharomi, O. O., Ngonghala, C., and Gumel, A. B. (2020). Mathematical modeling and analysis of covid-19 pandemic in nigeria. *medRxiv*.

Koo, J. R., Cook, A. R., Lim, J. T., Tan, K. W., and Dickens, B. L. (2022). Modelling the impact of mass testing to transition from pandemic mitigation to endemic covid-19. *Viruses*, 14(5).

Omar, O. A., Alnafisah, Y., Elbarkouky, R. A., and Ahmed, H. M. (2021). Covid-19 deterministic and stochastic modelling with optimized daily vaccinations in saudi arabia. *Results in Physics*, 28:104629.

QGIS Development Team (Version 3.20, 2021). *QGIS Geographic Information System*. QGIS Association.

Reiner, R., Barber, R., Collins, J., Zheng, P., Adolph, C., Albright, J., Antony, C., Aravkin, A., Bachmeier, S., Bang-Jensen, B., Bannick, M., Bloom, S., Carter, A., Castro, E., Causey, K., Chakrabarti, S., Charlson, F., Cogen, R., Combs, E., and Murray, C. (2021). Modeling covid-19 scenarios for the united states. *Nature Medicine*, 27.

Talekar, A., Shriram, S., Vaidhiyan, N., Aggarwal, G., Chen, J., Venkatramanan, S., Wang, L., Adiga, A., Sadilek, A., Tendulkar, A., Marathe, M., Sundaresan, R., and Tambe, M. (2020). Cohorting to isolate asymptomatic spreaders: An agent-based simulation study on the mumbai suburban railway.

Tang, Y. and Wang, S. (2020). Mathematic modeling of covid-19 in the united states. *Emerging Microbes & Infections*, 9(1):827-829. PMID: 32338150.

Wilder, B., Charpignon, M., Killian, J., Ou, H.-C., Mate, A., Jabbari, S., Perrault, A., Desai, A., Tambe, M., and Majumder, M. (2020). The role of age distribution and family structure on covid-19 dynamics: A preliminary

modeling assessment for hubei and lombardy. *SSRN Electronic Journal*.

Zhang, Y., You, C., Cai, Z., Sun, J., Hu, W., and Zhou, X.-H. (2020). Prediction of the covid-19 outbreak based on a realistic stochastic model. *medRxiv*.

